An Alternative Approach to the Executive Control of Root Piles

F.F. Monteiro, A.S. Moura, M.F.P. Aguiar

Abstract. A root pile is an injected type of pile (cast-in-place with pressure, with very distinct construction aspects from the known micropile type). Those piles are installed by using distinct injection pressures up to 500 kPa during the mortar shaft formation. The executive control of root piles is usually carried out by static load tests, requiring a costly and time-consuming assessment method. To study root pile performance, static load tests were performed on eight monitored piles with diameters of 350 and 410 mm. This paper proposes an alternative methodology for confirming the root pile performance based on the use of a speedometer attached to the rotatory head of the drill rig. The methodology consists in monitoring variables that are related to the pile bearing capacity, thus, proposing empirical equations with simple and applicable use to estimate root pile bearing capacity during installation. The results obtained by the proposed equations were in agreement with the values obtained from static load tests for the tested piles. Therefore, the results show that the methodology proposed presents itself as a viable alternative for the executive control of root piles.

Keywords: foundations, micropiles, piles, root piles, static load test.

1. Introduction

The recent increase in the size of construction works has boosted advances in foundation engineering. Pile foundations are one of the most important foundation techniques and are widely used in foundation engineering (Zhou *et al.*, 2018). With the technological evolution of equipment used in the construction of foundations, as well as the development of new types of foundations, the use of bored piles has become widely spread in great urban centers of Brazil. In this context, the growth of root piles as a foundation solution for construction works is notorious. The root pile is an injected type of pile (cast-in-place with pressure, with very distinct construction aspects from the known micro-pile type). Those piles are performed by using distinct injection pressures up to 500 kPa during the mortar shaft formation.

The performance assessment of deep foundations varies according to the pile type. In the case of root piles, the performance assessment is usually performed after pile execution, by carrying out static load tests. The static load test to failure is by far the most reliable method to determine both the bearing capacity and the load–settlement relationship of a pile. Consequently, the most significant progresses in the field of pile design have been obtained just by collecting and interpreting data from load tests (Russo, 2012). Although the static load test is easy to perform and interpret, it is expensive, slow to implement, and cannot be used systematically because it can destroy the micro-pile (Calvente *et al.*, 2017). Therefore, a shortage of alternatives that assist in performance assessment of root piles is identified. In order to overcome these disadvantages, this paper proposes an alternative methodology for confirming root pile erformance based on the use of a speedometer attached to the rotatory head of the drill rig. The methodology consists in monitoring variables that are related to the pile bearing capacity, thus, proposing empirical equations that are simple and can be used for estimating root pile bearing capacity during their installation. Then the methodology is tested and calibrated on real-scale root piles at several experimental sites where five root piles with lengths ranging from 7.7 to 26 m were installed. Finally, to validate the methodology, the results of the proposed equations are compared with static load tests carried out on three real-scale root piles. Many researchers have investigated root pile performance, and several significant conclusions have been made (Cadden *et al.*, 2004; Huang *et al.*, 2007; Moura *et al.*, 2015; Lima & Moura, 2016; Melchior Filho, 2018). Similar researches were carried out regarding different types of piles (Lin *et al.*, 2004; Herrera *et al.*, 2009; Basu *et al.*, 2010; Silva *et al.*, 2012; Silva *et al.*, 2014).

This research aims to propose a methodology for root pile installation control. For that purpose, three equations were proposed to estimate the pile bearing capacity (Q_{ult}), which allows to control the root pile execution process. The pile bearing capacity (Q_{ult}) is necessary to carry out perfor-

Fernando Feitosa Monteiro, Ph.D. Student, Departamento de Engenharia Civil e Ambiental, Campus Darcy Ribeiro, Universidade de Brasília, Brasília, DF, Brazil. e-mail: engffmonteiro@gmail.com.
Alfran Sampaio Moura, D.Sc., Associate Professor, Centro de Tecnologia, Campus do Pici, Universidade Federal do Ceará, Fortaleza, CE, Brazil. e-mail: alfransampaio@ufc.br.
Marcos Fábio Porto de Aguiar, D.Sc., Associate Professor, Instituto Federal de Educação, Ciência e Tecnologia do Ceará, Fortaleza, CE, Brazil. e-mail: marcosporto@ifce.edu.br.
Submitted on March 17, 2019; Final Acceptance on August 1, 2019; Discussion open until April 30, 2020.
DOI: 10.28927/SR.423289

mance control of the execution process. Thus, it is necessary to use an expression, or more than one that allow, Q_{ult} estimation, in order to verify the minimum pile length during pile installation. In the specific case of the equations proposed in this research, the procedure is performed with measurements of N_{SPT}, pile geometry, drill bit advance velocity and drill bit linear velocity.

2. Root Pile Installation Process

The root pile installation process is presented in Fig. 1. A rotary drilling technique was used to install the test root piles. First, the drill casing was attached to the rotary head, which rotates to advance the drilling into the soil or rock (Fig. 1a). After that, a drilling rod (inner rod) was attached to the same rotary head to perform the drilling inside the drill casing. The drilling rod advanced ahead of the tip of the casing. High pressure water jets were used to clear the cuttings as drilling advanced (Fig. 1b). At the final depth, the base was cleaned using high pressure water jets until no soil or rock cuttings were observed. After reaching the desired depth, the inner rod was removed, whereas the outer steel casing was left permanently in the ground. A rebar was then installed into the drilling hole (Fig. 1c). The casing was then filled with grout (0.6 water–cement ratio) until grout was flowing through the annulus between the drilled hole and the outer casing (Fig. 1d). A plug is installed at the drill casing upper end and pressure (compressed air) is applied while the drill case is removed. The diameter of the drilling bit used to drill the test piles is equal to 0.31 m (Fig. 2).

3. Proposed Methodology

The methodology proposed is based on the use of a digital speedometer to monitor variables during pile installation. First, the monitoring equipment is set up on the rotary head of the drill rig as shown in Fig. 3.

The drill rotator diameter is digitally inserted in the speedometer, in such a way that the sensor records each complete lap performed by the drill rotor (magnet). This procedure allows recording the linear distance traveled by the drill rotor for a determinate period of time. The drilling rod used to drill the last meter length of the pile was then, marked with sections of 10, 20 and 20 cm as seen in Fig. 4.

The elapsed time to drill the length between 2 marked sections was recorded in order to determine the advance velocity (V_a). The other measured variable is the drill rotator linear velocity (V_b), which is measured for the same section. The linear distance traveled by the drill rotor between 2 marked sections is divided by the circumferential length of the drill rotor, thus, obtaining the number of rotations performed by the drill rotor during the drilling of the mentioned section. From the elapsed time during the drilling of this section and the number of rotations performed by the drill rotator, it is possible to determine the number of rotations per minute, that is, the frequency (f) of the drill rotor. The drill rotor angular velocity (ω_r) is then, obtained from the following relation:

$$\omega_r = 2\pi f \tag{1}$$

Since the drill rotor is connected by the drilling rod to the drill bit at the bottom of drilling hole while the drilling is performed (Fig. 4), it can be assumed that the drill bit angular velocity (ω_b) is equal to the drill rotor angular velocity (ω_r).

$$\omega_r = \omega_b \tag{2}$$

The drill bit linear velocity (V_b) is then determined from the following equation:

$$V_b = \omega_b R_b \tag{3}$$

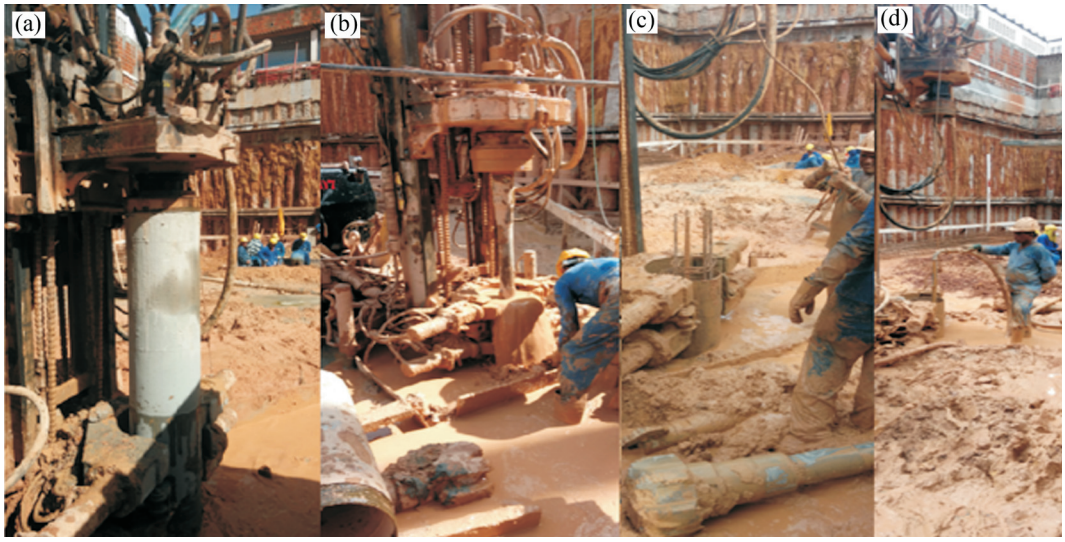

Figure 1 - (a) Drill case drilling, (b) drill rod drilling, (c) reinforcement bar installation, (d) grouting.

Figure 2 - Drill bit.

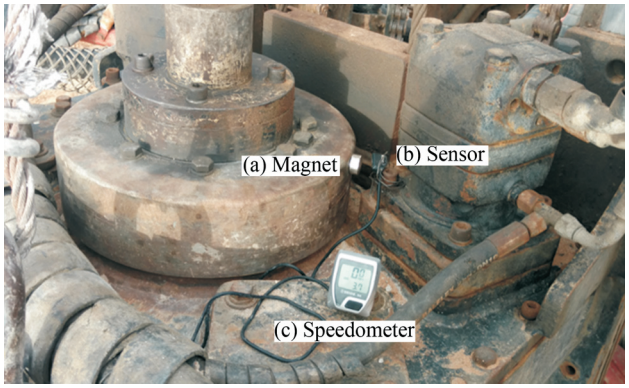

Figure 3 - Monitoring equipment. (a) Magnet, (b) Sensor, (c) speedometer.

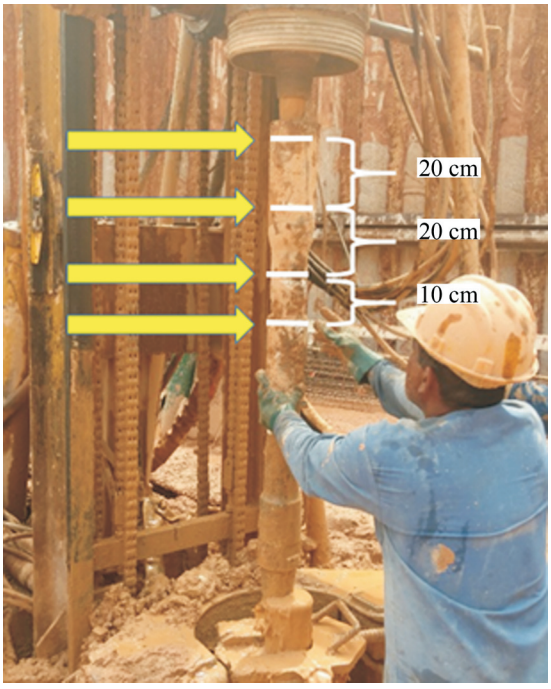

Figure 4 - Drilling rod marked sections.

where: V_b is the drill bit linear velocity; ω_b is the drill bit angular velocity and R_b is the drill bit radius.

Then, the drill bit linear velocity and the drill bit advance velocity are associated with the pile bearing capacity. The formulation of equations for executive control of the monitored test piles was initiated by choosing variables that would be used in the equation and considering that the formulation is intended to contribute to the development of an empirical approach with simple application in the executive control of root piles. Two variables obtained during monitoring were selected for correlating to pile bearing capacity: the drill bit linear velocity (V_b) and the drill bit advance velocity (V_a), the first one being associated to the skin friction resistance (Q_s) and the second to the tip resistance (Q_{tip}). In addition to the drill bit linear velocity (V_b) and drill bit advance velocity (V_a), the following variables were considered: tip resistance index ($N_{SPT,\ tip}$), average shaft resistance index ($N_{SPT,\ shaft}$), pile diameter (D), pile length (L), pile perimeter (U) and tip cross sectional area (A_p). The average shaft resistance index ($N_{SPT,\ shaft}$) is determined from the average N_{SPT} values along the pile shaft indicated in the standard penetration test results. The tip resistance index ($N_{SPT,\ tip}$) is determined by the average of the N_{SPT} values at the pile final depth indicated in the standard penetration test results.

Static load tests were carried out to determine the bearing capacity of the test piles. On most occasions, a distinct plunging ultimate load (Q_u) was not obtained in the test, and therefore, the Van der Veen extrapolation method was applied to obtain the ultimate load of the test piles (Van der Veen, 1953). In order to correlate the monitored variables and the pile ultimate load, it was necessary to estimate the load distribution along the pile shaft and tip. The Brazilian standard (ABNT, 2010) states that for bored piles, the load distribution must occur as 80 % to the pile shaft and 20 % to the pile tip. Since the static load tests were not instrumented, three distinct scenarios were proposed. In the first scenario, the load distribution would occur with 80 % along the pile shaft and 20 % at the pile tip. In the second scenario, the load distribution would occur with 90 % along the pile shaft and 10 % at the tip. Finally, in the third scenario, the load distribution would only occur along the pile shaft, that is, with 100 % along the shaft. In this way, the mentioned scenarios are presented as alternatives for use in practical cases. The definition of the expression to be adopted in real situations will depend on the user's own judgment, who may even apply the three equations to simulate possible real case scenarios.

For the development of the proposed equations in this paper, a multiple linear regression analysis method was used to explain the relationship between a dependent variable and several independent variables, so that:

$$Y = a_0 + a_1 X_1 + a_2 X_2 + \ldots + a_n X_n \quad (4)$$

where Y is the dependent variable (in this case, Q_{tip} or Q_s); X_1, X_2, ..., X_n are the independent variables; a_1, a_2, ..., a_n are the coefficients of the respective independent variables, known as regression coefficients and a_0 is a constant whose purpose is to represent the portion of Y that was not explained by the independent variables. By this approach and using the least squares method, the desired expression is adjusted based on the smallest deviation between the observed real values of the variable and the estimated value. Thus, considering a multiple linear function with three variables, the following system must be solved:

$$\sum Y = na_0 + a_1 \sum X_1 + a_2 \sum X_2 + a_3 \sum X_3 \quad (5)$$

$$\sum YX_1 = a_0 \sum X_1 + a_1 \sum X_1^2 + a_2 \sum X_1 X_2 + a_3 \sum X_1 X_3 \quad (6)$$

$$\sum YX_2 = a_0 \sum X_2 + a_1 \sum X_2 X_1 + a_2 \sum X_2^2 + a_3 \sum X_2 X_3 \quad (7)$$

$$\sum YX_3 = a_0 \sum X_3 + a_1 \sum X_3 X_1 + a_2 \sum X_3 X_2 + a_3 \sum X_3^2 \quad (8)$$

Using this system, the values of a_0, a_1, a_2 and a_3 are calculated using the current data of Y, X_1, X_2, X_3. As the relations between the variables are not linear in methods of bearing capacity estimation, it was necessary to use a logarithmic transformation of variables to create an exponential model. The following equations illustrate the procedure:

$$Y = a_0 \times X_1^{a_1} \times X_2^{a_2} \times \ldots \times X_n^{a_n} \quad (9)$$

$$\ln(Y) = \ln(a_0) + a_1 \times \ln(X_1) + a_2 \times \ln(X_2) + \ldots + a_n \times \ln(X_n) \quad (10)$$

Therefore, considering the new variables as ln (X_i) and solving the system of Eqs. 5 to 8, it is possible to use the logarithmic transformation of variables, then, apply the multiple linear regression model and obtain the values of the coefficients a_i.

Hence,

$$Q_u = Q_s + Q_{tip} \quad (11)$$

$$Q_{tip} = a_0' A_p^{a_1} V_a^{a_2} N_{SPT,tip}^{a_3} \quad (12)$$

$$Q_s = a_0'' V_b^{a_4} (UL)^{a_5} \overline{N}_{SPT,shaft}^{a_6} \quad (13)$$

where A_p is the tip cross sectional area; V_a drill bit advance velocity; ($N_{SPT, tip}$) is the tip resistance index; V_b is the drill bit linear velocity; U is the pile perimeter, L is the pile length; ($N_{SPT, shaft}$) is the average shaft resistance index; a_1, a_2, a_3, a_4, a_5, a_6 are linear regression coefficients; a_0' and a_0'' are regression constants.

4. Soil Profile and Site Description

Five construction sites were selected for this research; in all those sites, root pile foundations were built. In Fig. 5, the location of the selected sites for the development of the research is presented. The construction sites are located in the city of Fortaleza, Brazil.

SPTs and rock core borings were performed at five construction sites before installation of the root piles. In site 1, the groundwater level was found at a depth of 3 m. From the ground surface to 5 m, a clayey silt layer was encoun-

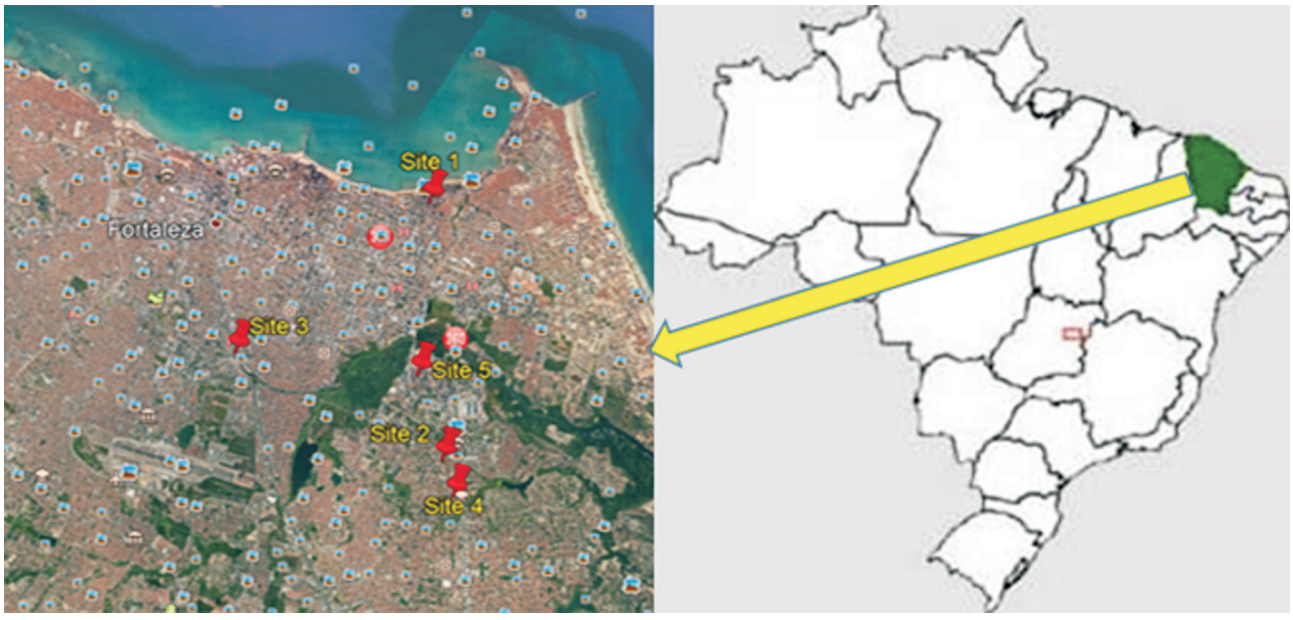

Figure 5 - Construction sites location.

tered, with *N* values ranging between 16 and 60. Below this layer, a sandstone layer with RQD varying from 43 to 54 % was encountered to a depth of 15 m; the *N* values, ranged from 58 to 60. In site 2, from the ground surface to 11 m, a clayey sand layer was encountered, with *N* values ranging between 3 and 60. Below this layer, a silty clay layer was encountered to a depth of 16 m; the *N* values ranged from 29 to 60. The bedrock is 16 m below the ground surface. The groundwater level was found at a depth of 1.2 m.

In site 3, the first layer with a total thickness of 2 m consists of silty sand soil, with *N* values ranging between 12 and 25. Below this layer, a silty clay layer was encountered to a depth of 11 m; the *N* values ranged from 38 to 60. Finally, a magmatic gneiss layer with RQD varying from 54 to 100 % was found to a depth of 26 m; the *N* values along this layer are equal to 60. The groundwater level was at a depth of 2 m.

In site 4, the groundwater level was found at a depth of 6.7-7.4 m. From the ground surface to 4 m, a silty sand layer was encountered with *N* values ranging between 2 and 4. Below this layer, a clayey sand layer was encountered to a depth of 12 m; the *N* values, ranged from 4 to 9. Finally, a sandy clay layer with *N* values varying from 9 to 42 was encountered to a depth of 22 m.

In site 5, the first layer with a total thickness of 11 m consists of silty sand soil, with *N* values ranging between 6 and 60. Finally, a clayey silt layer with *N* values varying from 7 to 59 was encountered to a depth of 19 m. The groundwater level was at a depth of 3.85 - 4 m.

Figures 6, 7, 8, 9, 10 and 11 present the geometry of the test root piles and the subsurface profile at the construction site locations.

5. Load-Displacement Test Results and Procedures

Static load tests were performed on the test piles 10 days after installation. The vertical settlement of the pile head was measured by four dial gauges (two on each side of the pile) attached to two reference beams. The load was applied in increments of 20 % of the final test load and maintained until the settlement rate from two consecutive settlement readings at the pile head was less than 5 %. After reaching the maximum load, the pile was unloaded in five load stages, with the exception of pile 6. In Table 1, the geometry of the tested piles, the maximum applied load, injection pressure and maximum recorded displacement are summarized. Figs. 12 and 13 show the applied load at the pile head *vs.* pile head settlement curves obtained from the static load tests.

The curves show that the tests on piles 6 and 8 fully mobilized the shaft friction, showing a sudden increase in the settlement at about the maximum applied load. The other tests were executed on piles with the same diameter (d = 0.41 m) but with different lengths: the piles are far from failure and exhibit similar behavior mainly governed by the shaft friction along the shaft. On most tests, a distinct plunging ultimate load (Q_u) was not obtained, and therefore, the Van der Veen extrapolation method was applied to obtain the ultimate load of the test piles. The extrapolated ultimate load (Q_u) values are presented in Table 2.

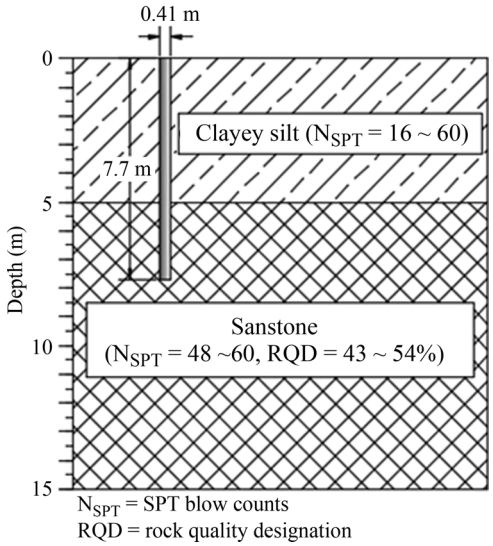

Figure 6 - Subsurface profile and test piles 1 and 2.

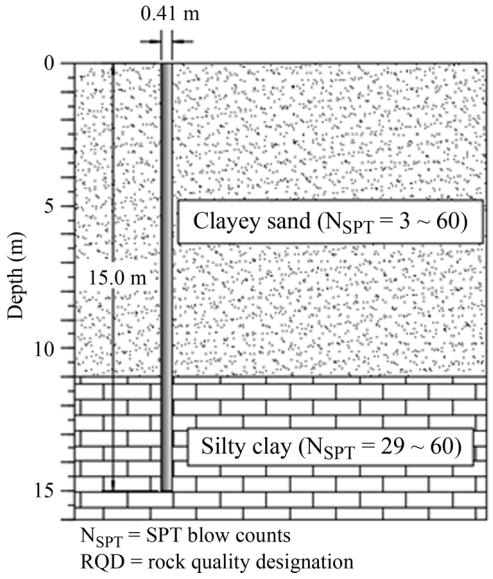

Figure 7 - Subsurface profile and test piles 3 and 4.

6. Monitoring Results

The monitoring process was performed during test pile installation. The data acquisition system (speedometer) recorded the drill bit linear velocity (V_b) and drill bit advance velocity (V_a) during the drilling of the marked sections on the drill rod. In Table 3, the monitoring results are presented. However, due to unforeseen events that occurred during field monitoring, it was necessary to perform changes in the lengths of the marked sections in some test piles.

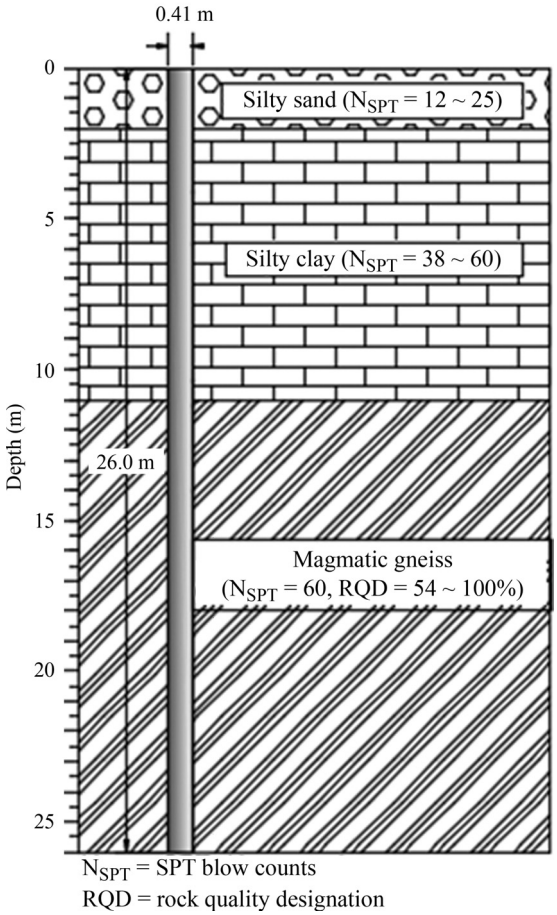

Figure 8 - Subsurface profile and test pile 5.

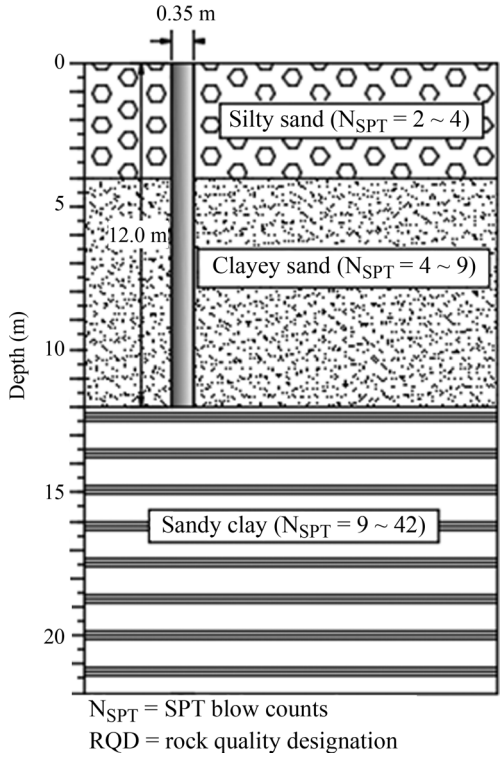

Figure 9 - Subsurface profile and test pile 6.

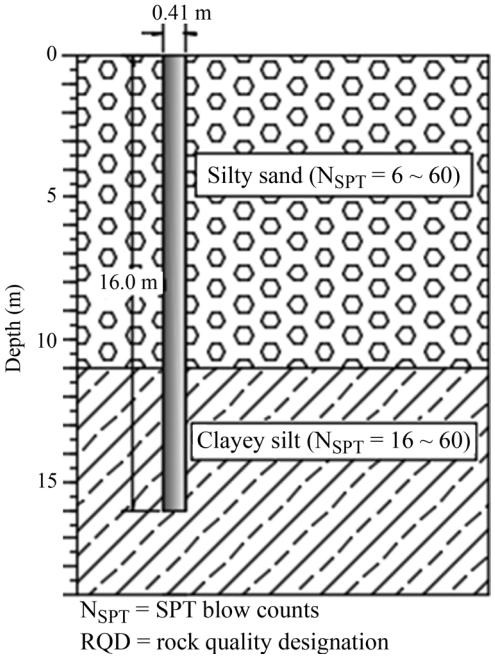

Figure 10 - Subsurface profile and test pile 7.

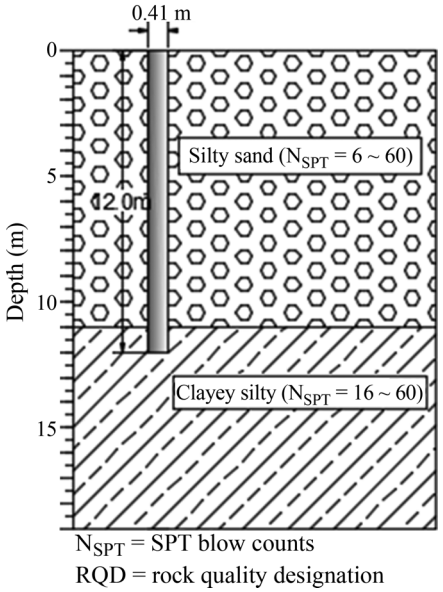

Figure 11 - Subsurface profile and test pile 8.

The penetration resistance index value (N_{SPT}) was limited to 60, in depths that presented high *N* values, in which the pile execution continued without additional difficulties.

For piles 1 and 2, executed in similar stratigraphic profiles (site 1), higher excavation times are observed when compared to the other piles, which is attributed to the pile tip being seated on a rock profile. Thus, for these piles, lower advance velocities are verified. However, the drill rotor frequency, which is directly associated with the drill bit

Table 1 - Summary of load test data.

Site	Test pile	*L* (m)	*D* (m)	Applied load (kN)	Settlement (mm)	Injection pressure (kPa)
1	1	7.7	0.41	2000	2.24	400
2	7.7	0.41	2000	4.32	400	
2	3	15	0.41	2400	11.24	300
4	15	0.41	2400	10.38	300	
3	5	26	0.41	2240	8.04	300
4	6	12	0.35	1620	15.61	300
5	7	16	0.41	2400	13.85	300
8	12	0.41	2400	25.04	300	

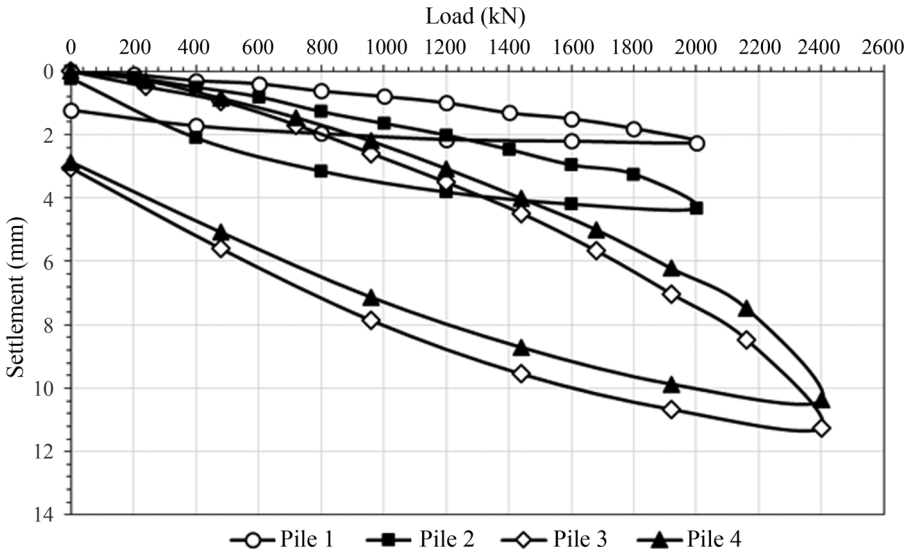

Figure 12 - Results from static load tests on piles 1, 2, 3 and 4.

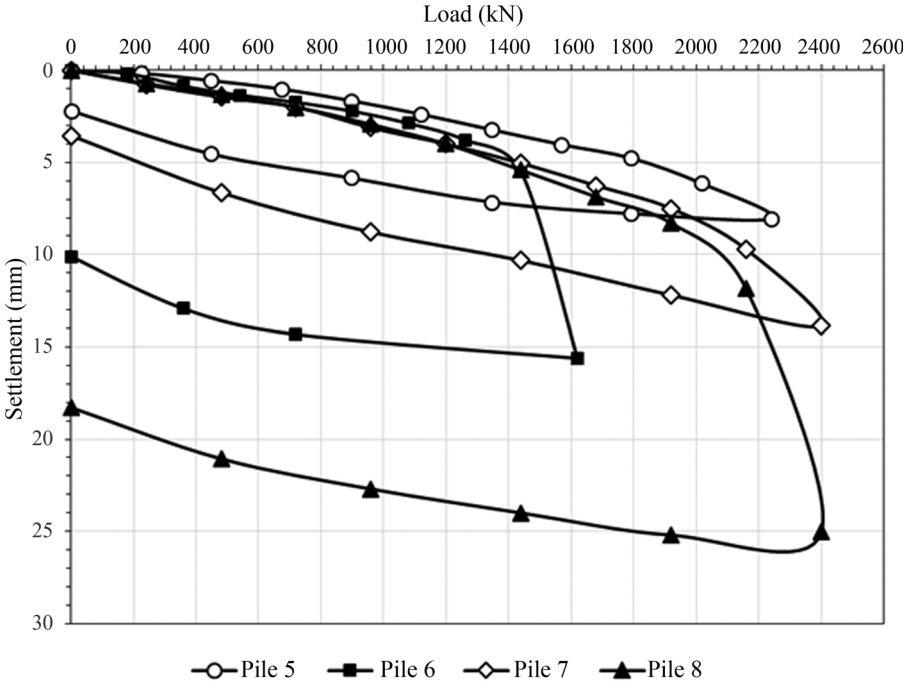

Figure 13 - Results from static load tests on piles 5, 6, 7 and 8.

Table 2 - Extrapolated ultimate load (Q_u) values.

Site	Pile	Q_u (kN)
1	1	3000
	2	3200
2	3	3100
	4	2900
3	5	2800
4	6	1550
5	7	2450
	8	2150

linear velocity, presents similar values when compared with values for piles 4 and 5.

Pile 5 (site 3), which has the tip supported in magmatic gneiss, presents an average penetration resistance index along the shaft similar to piles 1 and 2, which also have the tip supported on rock. In site 4, where pile 6 was executed, a reasonable compliance with pile 8 is verified when advance velocity is evaluated. Piles 6 and 8 are embedded in soils whose stratigraphy alternates between clayey silt, silty sand, clayey sand and sandy clay. These piles present a 7.4 % variation when compared to the respective advance velocities, which is smaller for pile 8. This is due to the fact that the penetration resistance index at the tip of pile 8 is higher than for pile 6. Thus, a correlation between these two variables is observed, in such a way that the higher the penetration resistance index, the lower the advance velocity, noting an inversely proportional ratio. High frequency values were observed during installation of piles 6, 7 and 8, which were already expected due to the direct frequency relationship with the drill bit linear velocity (V_b). Thus, it is possible to observe, that the higher the frequency, the greater the drill bit linear velocity and the smaller the soil *N* value. Based on the above, it is possible to infer that pile load capacity is inversely proportional to the drill bit linear velocity (V_b) and the frequency. Table 4 shows the average values of the monitored variables and the ultimate load for each test pile.

Table 3 - Monitoring results.

Pile	Drilled length (m)	Time (s)	V_a 10^{-3} (m/s)	Frequency (Hz)	ω_b (rad/s)	V_b (m/s)	$N_{SPT, tip}$	$N_{SPT, shaft}$
1	0.1	38.00	2.63	2.01	12.60	1.95	60	50
	0.2	51.00	3.92	2.50	15.72	2.44		
	0.2	78.00	2.56	2.15	13.50	2.09		
	0.2	72.00	2.78	2.25	14.13	2.19		
2	0.1	27.00	3.70	1.76	11.08	1.72	60	52
	0.2	50.00	4.00	2.67	16.76	2.60		
	0.2	56.00	3.57	1.36	8.55	1.33		
	0.2	54.00	3.70	2.65	16.62	2.58		
3	0.1	11.22	8.91	2.55	16.00	2.48	60	33
	0.1	8.27	12.10	1.15	7.24	1.12		
	0.2	19.28	10.40	0.99	6.21	0.96		
4	0.1	4.76	21.00	2.00	12.57	1.95	60	32
	0.2	9.78	20.40	1.95	12.24	1.90		
	0.2	15.84	12.60	1.20	7.56	1.17		
5	0.1	18.59	5.38	1.54	9.66	1.50	60	52
	0.2	34.30	5.83	1.94	12.21	1.89		
	0.2	43.19	4.63	1.76	11.08	1.72		
6	0.15	29.00	5.20	3.99	25.10	3.89	10	6
	0.2	43.00	4.70	4.06	25.48	3.95		
7	0.3	30.00	1.00	2.05	12.86	1.99	39	22
	0.2	27.00	7.40	2.44	15.32	2.37		
8	0.3	38.00	7.90	1.61	10.14	1.57	22	22
	0.2	44.00	4.50	4.38	27.52	4.27		

7. Equations Proposal and Validation

For the development of the equations, a multiple linear regression analysis method was used. Initially, piles 3, 4, 6, 7 and 8 were chosen for the development of the expression (calibration), then piles 1, 2 and 5 were chosen for validation. The selection of the piles for the calibration and validation of the equations was carried out randomly. As mentioned on a previous section, three distinct scenarios were proposed. In the first scenario, the load distribution would occur with 80 % along the pile shaft and 20 % on the pile tip. In the second scenario, the load distribution would occur with 90 % along the pile shaft and 10 % on the tip. Finally, in the third scenario, the load distribution would only occur along the pile shaft, that is, with 100 % along the shaft. The equations for the proposed scenarios are now, presented:

$$Q_{u,80/20} = \frac{81{,}61 A_p^{0,015} N_{SPT,tip}^{0,404}}{V_a^{0,08}} + \frac{1615{,}33 (UL)^{0,0058} \overline{N}_{SPT,shaft}^{0,168}}{V_b^{0,44}} \quad (14)$$

$$Q_{u,90/10} = \frac{40{,}80 A_p^{0,015} N_{SPT,tip}^{0,404}}{V_a^{0,08}} + \frac{1817{,}25 (UL)^{0,0058} \overline{N}_{SPT,shaft}^{0,168}}{V_b^{0,44}} \quad (15)$$

$$Q_{u,100/0} = \frac{2019{,}17 (UL)^{0,0058} \overline{N}_{SPT,shaft}^{0,168}}{V_b^{0,44}} \quad (16)$$

where A_p is the tip cross sectional area; V_a is the drill bit advance velocity; ($N_{SPT,\ tip}$) is the tip resistance index; V_b is the drill bit linear velocity; U is the pile perimeter, L is the pile length; ($N_{SPT,\ shaft}$) is the average shaft resistance index.

Analyzing the equations, it is verified that the regression coefficients did not change, whereas the regression constants changed; this occurred for both the skin friction bearing capacity and the tip bearing capacity. The regression constant of skin friction bearing capacity gradually increased when moving from one scenario to the other. The coefficient of determination (R^2) of the equations is 0.99.

It is noteworthy that the equations proposed for the executive control present physical sense for the pile ultimate load capacity, and the variables that have a positive regression coefficient, are directly proportional to the pile bearing capacity. Thus, for example, the greater the pile perimeter (U), pile length (L) or average shaft resistance index ($N_{SPT,\ shaft}$), the greater the pile skin friction bearing capacity. On the other hand, the greater the drill bit linear velocity (V_b), the lower the pile skin friction bearing capacity. The methodology proposed was verified on root piles monitoring data that were not part of the universe used for the development of the equations by comparing the results obtained from load tests performed on these piles and values obtained from the proposed equations. Piles 1, 2 and 5 were randomly selected to carry out the validation. The proposed equations did not consider the injection pressure. However, Melchior Filho (2018) observed the small influence of this variable in the evaluation of Q_{ult}. More details are presented in Melchior Filho (2018). It is also important to point out that the injection pressure of all the piles chosen for the development of the expression (calibration) was about 300 kPa. Table 5 shows the load capacity estimates from the proposed expressions, as well as those obtained from the load tests.

Considering the presented scenarios, it is observed that the percentage error between the estimated values and the reference values considered was at least 2.8 % and at most 13.3 %. When comparing the estimated pile bearing capacity values and the reference values for pile 1, an absolute error of 4.6 % is verified. It is worth mentioning that all bearing capacity estimates for pile 1 presented values slightly lower than the reference value (ultimate load obtained from the load test). For pile 2, an absolute error of

Table 4 - Average monitoring variables values.

Pile	Drilled length (m)	Time (s)	V_a 10^{-3} (m/s)	Frequency (Hz)	ω_b (rad/s)	V_b (m/s)	$N_{SPT,\ tip}$	$N_{SPT,\ shaft}$	Q_u (kN)
1	0.175	59.75	2.97	2.23	13.99	2.17	60	50	3000
2	0.175	46.75	3.74	2.11	13.25	2.05	60	52	3200
3	0.133	12.92	10.50	1.56	9.81	1.52	60	33	3100
4	0.167	10.13	18.00	1.72	10.79	1.67	60	32	2900
5	0.167	32.03	5.28	1.75	10.98	1.70	60	52	2800
6	0.175	36.00	4.95	4.03	25.29	3.92	10	7	1550
7	0.25	28.50	8.70	2.24	14.09	2.18	39	22	2450
8	0.25	41.00	6.20	3.00	18.83	2.92	22	22	2150

Table 5 - Methodology validation.

Method	Pile 1			Pile 2			Pile 5		
	Q_s (kN)	Q_{tip} (kN)	Q_u (kN)	Q_s (kN)	Q_{tip} (kN)	Q_u (kN)	Q_s (kN)	Q_{tip} (kN)	Q_u (kN)
Q_u, 80/20	2244	671	2915	2314	658	2972	2533	639	3173
Q_u, 90/10	2525	335	2860	2603	329	2932	2850	319	3170
Q_u, 100	2805	0	2805	2893	0	2893	3167	0	3167
Load test Q_u (kN)		3000			3200			2800	

8.3 % is observed when comparing the pile bearing capacity values with the reference values. As for pile 1, it is found that the bearing capacity values predicted for pile 2 are lower than the reference values; this occurs for all load distribution scenarios. A distinct trend is verified for pile 5, with the greater absolute error (average of 13.2 %). The pile bearing capacity values predicted for pile 5 were higher than the reference value.

It is important to mention that the use of the SPT on fine soils has some limitations, due to the characteristics of the test, in which a great disturbance of the soil structure is observed. Eurocode 7 states that the use of the SPT should be restricted to a qualitative evaluation of the soil profile as there is no general agreement on the use of SPT results in clayey soil (BS, 2007). The soil profiles analyzed to develop the proposed methodology consist, mostly, of coarse soils. Therefore, the application of this methodology to clayey soils has to be performed with proper evaluation. It is worth mentioning that the use of the proposed equations is restricted to soils with similar characteristics to those of this research. In this sense, the use of the proposed expressions in fine soil profiles should be preceded by further research, in order to contemplate a wider range of soil types.

In general, the bearing capacity values estimated by the proposed equations were in agreement with the reference values. Therefore, a correlation between the pile bearing capacity and the suggested variables is observed. It is worth mentioning that the proposal of this work is to present a simplified procedure for the executive control of root piles, helping in the decision-making during field execution, in relation to the definition of the pile length to be executed.

8. Conclusions

In this research, simplified methodologies and equations for the executive control of root piles were proposed, providing a useful tool to assist in the decision-making during field execution. The methodology is based on the monitoring of execution variables (advance velocity and drill bit linear velocity), determined from fundamentals of classical physics with measurements made during field testing. Based on these equations, it became possible to establish a monitoring methodology for root piles. The measured execution variables during monitoring are correlated with ultimate load values obtained from load tests.

This methodology is easy to carry out and provides an immediate interpretation. The methodology allows a systematic control without disturbing root piles. It is also adapted to the real conditions of root pile construction sites and is therefore a technically and economically feasible methodology. At present, the methodology is limited to root piles having a length lower than 30 m and maximum bearing capacity of 3500 kN. This methodology can provide the ultimate bearing capacity of the pile with a reasonable accuracy.

This alternative and original methodology has the advantage of estimating the root pile bearing capacity during pile installation with a non-destructive approach. This means that in the absence of a static load test, the methodology can become an alternative for the root pile executive control. The monitoring protocol and the processing and treatment of the acquired data show that the methodology proposed can provide results with great similarity when compared to static load test results.

Acknowledgments

This research was carried out under the auspices of the Foundation Group (M.Sc., Professors and Technicians) of the Geotechnical Post-Graduation Program of the University of Ceará-UFC (POSDEHA/UFC). The authors would like to express their gratitude to the engineering contractors FUNDAÇÕES GEOBRASIL and TECNORD for the field support, and to the Governmental sponsorship organization CAPES for the scholarship provided to the first author.

References

ABNT, Brazilian Association of Technical Standards (2010). Foundation Design and Execution. NBR 6122-2010. Rio de Janeiro, Brazil, 91 p.

Basu P.; Prezzi M. & Basu D. (2010). Drilled displacement piles – Current practice and design. DFI Journal, 4(1):3-20.

BS, British Standard (2007). Eurocode 7 – Geotechnical Design – Part 2: Ground Investigation and Testing. British Standard Institution. London, England, 199 p.

Cadden, A.; Gomez J. & Bruce D. (2004). Micropiles: recent advances and future trends. Proc. Current practices and future trends in deep foundations, ASCE. Los Angeles, pp. 140-165.

Calvente, R.; Breul P.; Benz M.; Bacconet C. & Gourves R. (2017). Methodology for confirming the micropiles service performance based on dynamic tests. Journal of Geotechnical and Geoenvironmental Engineering, 143(5):040161231-040161238.

Herrera, R.; Jones L.E. & Lai P. (2009). Driven concrete pile foundation monitoring with embedded data collector system. Proc. International Foundation Congress and Equipment Expo, ASCE. Orlando, pp. 78-84.

Huang, Y.; Hajduk E.L.; Lipka D.S. & Adams J.C. (2007). Micropile load testing and installation monitoring at the CATS vehicle maintenance facility. Proc. Geo-Denver. Denver, ASCE, pp. 28-38.

Lin, G.; Hajduk E.L.; Lipka D.S. & NeSmith W. (2004). Design, monitoring, and integrity testing of drilled soil displacement piles (DSDP) for a gas-fired power plant. Proc. GeoSupport Conference. Orlando, pp. 17-29.

Lima, D.R.; & Moura, A.S. (2016). Executive control of root piles from field measurements. Ciência & Engenharia, 25:95-104 (In Portuguese).

Melchior Filho, J. (2018). Improvements Development for the Root Piles Executive Control Procedure of the Post-Graduation Program in Civil Engineering of the Federal University of Ceara. Masters Dissertation, Hydraulic and Environmental Engineering Department, Federal University of Ceará Fortaleza, 114 p. (In Portuguese).

Moura, A.; Lima, R. & Monteiro, F. (2015). A preliminary proposal: Executive control of root piles. The Electronic Journal of Geotechnical Engineering, 20(26):12906-12920.

Russo, G. (2012). Experimental investigations and analysis on different pile load testing procedures. Acta Geotechnica, 8(1):17-31.

Silva, C.M.; Brasil A.L. & Camapum de Carvalho, J. (2012). On modelling coninuous flight auger pilings by means of energy. International Journal of Science and Engineering Investigations, 1:11-16.

Silva, C.M.; Camapum de Carvalho, J. & Brasil, A.L. (2014). The SCCAP methodology applied to design continuous flight auger pilings. The Electronic Journal of Geotechnical Engineering, 19(4):16909-16919.

Van der Veen, C. (1953). The bearing capacity of a pile. Proc. Third International Conference on Soil Mechanics and Foundation Engineering, Zurich, v. II, pp. 84-90.

Zhou, J.; Gong, X.; Wang, K. & Zhang, R. (2018). Shaft capacity of the pre-bored grouted planted pile in dense sand. Acta Geotechnica, 13(5):1227-1239.